ELSEVIER

Biophysical Chemistry 94 (2001) 175–184

Biophysical Chemistry

www.elsevier.com/locate/bpc

Torsional constant of 27-mer DNA oligomers of different sequences

Francesco Pedone[a], Filomena Mazzei[b,*], Mirella Matzeu[b], Flavia Barone[b]

[a] *Istituto Nazionale di Fisica della Materia, Università La Sapienza, Rome, Italy*
[b] *Laboratorio di Fisica, Istituto Superiore di Sanità, Viale Regina Elena 299, 00161 Rome, Italy*

Received 27 July 2001; received in revised form 17 September 2001; accepted 19 September 2001

Abstract

We have studied the torsional elastic constant (α) of short DNA (27mer) oligomers of various sequence by fluorescence polarization anysotropy (FPA) measurements. The lowest α values were found in samples with sequence rich in AA dinucleotides or containing the alternating d(A–T)·d(A–T) motif. The torsional rigidity of our DNA samples was compared to that calculated according to the current values of twist angle fluctuations derived for ten dinucleotide steps by recent analyses of DNA crystal structure database. The values of torsional rigidity derived from crystals are higher than our experimental ones, obtained by FPA analysis, suggesting that packing force in crystals may notably hinder the dinucleotide twist angle fluctuations that occur in solution. This behaviour is more evident for samples containing AA, TA and AT steps. In all the samples there is about a twofold change of the α value in the 10–40 °C range. An activation enthalpy ($\Delta H^{\#}$) of about 17.4 kJ mol^{-1}, on average, was obtained for the temperature dependence of eight of the ten samples studied. A correlation with the stacking energy is discussed.

Keywords: Fluorescence polarization anisotropy; Base stacking; Dinucleotide step rigidity

* Corresponding author. Tel. +39-6-4990-2612; fax +39-6-4938-7075.
E-mail address: mazzei@iss.it (F. Mazzei).

0301-4622/01/$ - see front matter
PII: S0301-4622(01)00232-0

1. Introduction

Among the mechanical properties of DNA, torsional rigidity is important to characterize the flexibility of this macromolecule. The dependence of torsional rigidity on base composition has been analyzed by fluorescence depolarization measurements conducted on different DNA forms [1,2] and small sequence effects were usually observed. The length of analyzed DNA was mainly high, beyond 1 K base, and short oligonucleotides more recently subjected to investigation [3–5] were not subjected to a systematic research, as far as sequence effects are concerned.

Long DNA fragments have also been used to study the temperature dependence of DNA torsional constant (α). Delrow et al. [6] observed a slight decrease of α with slight increase of the temperature from 5 to 60 °C, that was attributed to changes in secondary structure. We have recently studied by FPA several short synthetic oligonucleotides [5,7,8] also in form of RNA and hybrid RNA–DNA [9], and we have been able to evaluate the temperature dependence of the torsional constants. Now we have planned a systematic analysis of the sequence dependence of the torsional rigidity in short synthetic oligonucleotides. Furthermore, the temperature dependence of the torsional constant of these samples was investigated to allow the determination of the enthalpic term of the elastic torsional energy. The experimental data of the torsional rigidities obtained in solution for our samples were compared with those calculated by the crystal database for the dinucleotide steps [10–13].

2. Materials and methods

2.1. Oligonucleotide preparation

Twenty-seven base purified oligonucleotides were purchased from Boehringer and checked by us for length homogeneity by denaturing gel electrophoresis [14]. Generally, the fraction of full length oligonucleotides was more than 97%, so that they were used without any further purification. The concentration of single strands was determined spectrophotometrically with molar extinction coefficients calculated by using nearest neighbour analysis [15]. Fig. 1 reports the sequence and the order number of the ten samples. Duplexes were obtained by annealing the complementary strands, by mixing equimolar amounts of the oligonucleotides, heating at 90 °C for 10 min and then slowly cooling them at 4 °C. The purity of our duplex samples was checked by 15% polyacrylamide gel analysis in non denaturing conditions [14]. In the following the duplexes, always studied in 10 mM Na phosphate buffer 100 mM NaCl 0.1 mM EDTA pH 7.0 (buffer A), are denoted by the number shown in Fig. 1.

	5'	3'
1	GGC AAA AAA AAA AAA AAA AAA CGG	
2	GCT AAA AAA AAA AAG AGA GAG AGA TCG	
3	GGC ATA TAT ATA TAT ATA TAT ATA CGG	
4	GGC CGC GCG CGC GCG CGC GCG CGC CGG	
5	GAG GAA GGA AGG AAT CTC TCT CTC TCT	
6	ACG TGC ATG CAC ATA CAT GCG TAC ATG	
7	ACG TGC GTG CAC ATA CAT GCG TAC ATG	
8	AGG CTC GGA TCC AAA TCT AGA CTC AGA	
9	AGG CTC AGA TCC AGA TCT AGA CTC AGA	
10	GAA GAA GAG AAG GAA GGG AGA GGA AGA	

Fig. 1. Sequence of the ten samples studied. Only one strand of the duplexes is shown.

2.2. Premelting measurements

Circular dichroism (CD) measurements were performed by means of a Jasco spectropolarimeter equipped with a Peltier-type temperature control system (Jasco, Model PTC 348 WI). The samples were placed in 3 ml rectangular quartz cell with a path length of 1 cm. Spectra were automatically recorded at 5 °C intervals within the 5–80 °C range between 320 and 220 nm with a scanning rate of 10 nm/min. The spectral resolution was 0.2 nm and the band width 1 nm. In

addition, fine monitoring of the duplex melting transition was followed, during spectra acquisition, recording the changes in ellipticity at 250 nm every 0.2 °C. The temperature rate increase was about 0.5 °C/min.

2.3. UV thermal denaturation measurements

UV absorption changes at 260 nm (A) as a function of temperature were followed by means of a Cary 3 UV–vis spectrophotometer. The temperature was controlled by a Peltier device and raised at a rate of 0.5 °C/min in the range 5–95 °C. The samples, dissolved in buffer A at a concentration of about 5 nM, were placed in a 1-ml quartz cuvette with 1 cm path length. Absorbance values at 260 nm were corrected for water thermal expansion and normalized at the value of 1 optical density at the lowest temperature. Thermodynamic analysis was performed according to Breslauer [16]. The following parameters were derived: the melting temperature: T_m; the enthalpy change: ΔH_m; the cooperativity of the transition, described by the interquartile range (IR). This latter parameter was deduced taking into account the value of dA/dT at the melting point, and evaluating the width of the distribution at the values corresponding at 2/3 of the peak height.

2.4. Dynamic fluorescence measurements

Lifetimes and fluorescence polarization anisotropy measurements were carried out by means of a frequency domain fluorometer (K2-ISS, Urbana Illinois, USA). The duplexes, at a concentration of 0.6 mM of oligonucleotide, were dissolved in the buffer A and ethidium bromide (EB) added at a ratio of 1 mole of EB per 300 base pairs, in order to avoid energy transfer phenomena. Temperature control was by a circulating water bath (Haake K15) and the temperature of the block, containing the sample cuvette, was continuously monitored during the measurements in the range 4–40 °C with an Ellab probe (Ellab A/S, Roedovre, Denmark).

Dye fluorescence emission was excited with the 514 nm 0.5 W output of a Coherent Innova 90C argon laser. The modulation ratio of the excitation light was always in the range 60–70% and the detection cross correlation frequency was 80 Hz. A detailed report of the experimental setting is given elsewhere [7].

Lifetime determination between 4 and 40 °C was carried out in all the samples at each temperature before performing the corresponding anisotropy measurements. For the lifetime measurements, 10 frequencies logarithmically spaced in the 2–40 MHz interval were acquired. The excitation polarizer was set at 36° with respect to vertical polarization of the laser and polystyrene latex was used as reference. The data were analysed with the K2-ISS fluorometer software, using the lifetime value of free ethidium equal to 1.7 ns. The lifetime vs. temperature data were fitted by linear regression and this dependence was accounted for in the following FPA data analysis.

Anisotropy data were acquired at 20 frequencies in the 2–40 MHz interval with the excitation polarizer kept fixed at 0° (i.e. vertical) and the emission polarizer automatically rotated at 0 and 90° for each acquisition. The error for phase and modulation ratio was 0.2 and 0.004°, respectively, amounting to 1% of the signal.

The decay of fluorescence anisotropy is well described by the product of correlation functions, which are referred to the motions of the nucleic acids themselves [17]:

$$r(t) = \frac{I_{\parallel} - I_{\perp}}{I_{I_{\parallel}} + 2I_{\perp}} = r_0 \sum_{n=-2}^{2} A_n(t) C_n(t) F_n(t) \quad (1)$$

where r_0 is the EB limiting anisotropy value, which is usually found equal to 0.36. A_n are the internal correlation functions which are fully described by trigonometric functions of the angle θ formed by the EB dipole and the helical axis, which has been assumed to be equal to 70.5° [17]. $C_n(t)$ and $F_n(t)$ are the torsional and the bending correlation functions, respectively [17]. Due to the very short length of our samples bending motions were negligible.

In the frequency domain, the quantities usually measured to characterise the fluorescence polarization anisotropy decay are the difference between the phase angles (Φ) of the two components, parallel and perpendicular, with respect to the excitation beam, and the demodulation (M) ratio, according to:

$$\Delta\Phi = \Phi_{\perp} - \Phi_{\parallel} \tag{2}$$

$$\Delta\Lambda = M_{\parallel}/M_{\perp}$$

These quantities are related to the time decay of the fluorescence intensity (I) [3], as measured when the relative orientation of the excitation polarizer and the emission analyser are parallel ($I_{\parallel}$) or orthogonal ($I_{\perp}$), by means of Laplace transforms.

The Laplace transforms:

$$f_p(\omega) = \int_0^{\infty} \mathrm{d}t I_p(t) \mathrm{e}^{i\omega t} = L(I_p)(i\omega) \tag{3}$$

where $p = \parallel$ or $p = \perp$ were computed and combined as:

$$\Delta(\omega) = \mathrm{arctg}\frac{\mathrm{Im}(f_{\perp})\mathrm{Re}(f_{\parallel}) - \mathrm{Re}(f_{\perp})\mathrm{Im}(f_{\parallel})}{\mathrm{Re}(f_{\perp})\mathrm{Re}(f_{\parallel}) + \mathrm{Im}(f_{\perp})\mathrm{Im}(f_{\parallel})} \tag{4}$$

and:

$$\Lambda(\omega) = |f_{\perp}(\omega)|/|f_{\parallel}(\omega)|$$

Phase differences and demodulation ratios in the FPA measurements were fitted with a Vax station in order to obtain the hydrodynamic parameters. During the fitting procedure the elastic torsional constant α, the hydrodynamic radius R_h and the rise b were the free parameters.

3. Results and discussion

3.1. Samples characterization

The samples reported in Fig. 1 were constructed to represent: (i) the presence of repetitive AA steps as no. 1 and 2; (ii) the presence of alternating d(A–T)·d(A–T) and d(C–G)·d(C–G) motives as nos. 3 and 4; (iii) a single base substitution, as in sample nos. 6 and 7, at 7 position; (iv) two base substitutions as in samples nos. 8 and 9, at 7 and 14 positions; (v) the presence of long or total purine tract on one strand as in sample nos. 5 and 10.

UV thermal melting was performed on these samples and data of melting temperature T_m, of the interquartile temperature range (IR), and of the enthalpy change ΔH_m are reported in Table 1. It is evident from the table that the samples we are studying are very stable in the temperature range where the FPA and lifetimes measurements were performed. This observation ensures that the dye is, also at the higher temperature employed, bound to the duplexes and can well represent the DNA fragment internal motions. The enthalpy changes were reported in the same table only to further confirm that we are looking at fully annealed samples, as the values are comparable with those obtained by measuring DNA fragments of similar length.

Circular dichroism spectra revealed that all the samples assume in solution a B-DNA form. The presence of a premelting transition, in the temperature range 10–40 °C, was observed in sample nos. 1, 2 and 8 as reported in the same table.

3.2. Lifetime measurements

We have measured the fluorescence lifetime of the intercalated ethidium bromide (τ_{bT}) in the temperature interval between about 10–40 °C. The temperature dependence of the lifetime was fitted by a linear equation $\tau_{bT} = \tau_{b0} - kT$ with about the same slope k for all the samples and this dependence was used to fit the depolarization experimental data.

Table 2 reports, for each sample, the lifetime of the bound EB at 20 °C and the linear regression parameters. As can be seen the lifetime of EB varies from about 20 to 25 ns (sample nos. 2 and 3, respectively), showing the preference of EB for AT steps as reported in the literature [18,19]. The curves of samples 6 and 7 are almost coincident

Table 1
Thermal and thermodynamic parameters of the ten oligomers

Sample	T_m (°C)	IR (°C)	$-\Delta H_m$ (kJ/mol)	Premelting transition
1	56.0 ± 0.5	46–57	573 ± 59	+
2	61.5 ± 0.5	49–75	489 ± 50	+
3	48.3 ± 0.5	41–53	435 ± 42	−
4	> 90			−
5	65.2 ± 0.5	57–69	636 ± 63	−
6	67.5 ± 0.5	57–72	644 ± 63	−
7	72.2 ± 0.5	61–75	531 ± 54	−
8	68.7 ± 0.5	57–73	565 ± 58	+
9	67.2 ± 0.5	54–70	468 ± 46	−
10	63.7 ± 0.5	51–67	589 ± 58	−

T_m, IR and ΔH_m were derived from UV thermal analysis; the presence of the premelting transition was investigated by CD thermal analysis.

within the errors. In these samples the substitution of one A with a G has not varied the EB intercalation site. On the contrary a variation of the binding site may have occurred in the samples 8 and 9, probably upon the substitution at the boundary of the AAA tract.

3.3. Fluorescence polarization anisotropy measurements

In Fig. 2 the curves of the temperature dependence of the torsional constant α are shown. We used the exponential equation $\alpha(T) = \alpha_0 \cdot e^{-\Delta H^{\#}/RT}$ to fit the experimental data, where $\Delta H^{\#}$ is the activation enthalpy of the process, R is the gas constant and T the absolute temperature.

In Table 3 the dynamic parameters obtained by FPA analysis of the samples are reported. The values of the hydrodynamic radius R_h and rise b are consistent with those usually found by this technique for B-DNA forms and the values we report were found constant in the temperature range 10–40 °C. Good χ^2 values around 1 were usually found, never exceeding 1.2.

In Table 3, the $\Delta H^{\#}$ values and the α values extrapolated at 293 K for each sample are reported.

The $\Delta H^{\#}$ values range from 9.2 to 19.2 kJ/mol, i.e. a very low amount of energy that does not exceed the value of one hydrogen bond. What is under study by means of our FPA investigation are the thermal fluctuations of twist in a short temperature interval where no particular transi-

Table 2
Lifetimes at 20 °C of DNA bound ethidium bromide and lifetime temperature dependence

Sample	τ_{b20} (ns) (± 0.2)	$\tau_{bT} = \tau_{b0} - kT$ (ns)
1	21.2	$22.0-0.04T$
2	20.3	$21.2-0.05T$
3	25.2	$26.5-0.07T$
4	22.3	$23.2-0.07T$
5	21.1	$22.1-0.05T$
6	24.4	$25.6-0.06T$
7	24.2	$25.4-0.06T$
8	22.1	$22.9-0.04T$
9	22.6	$23.6-0.05T$
10	21.1	$21.9-0.04T$

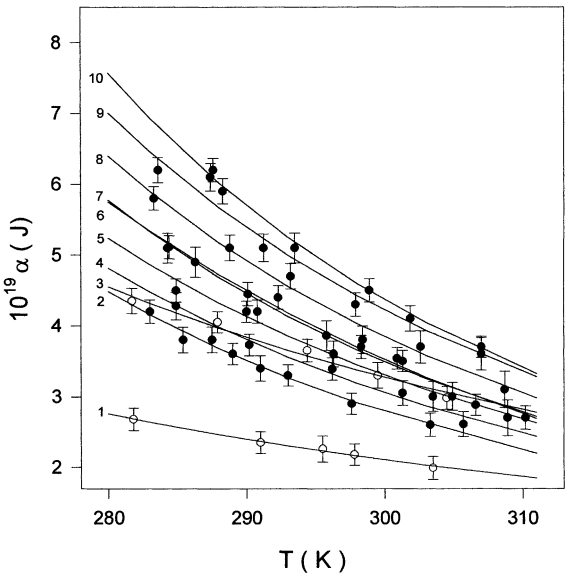

Fig. 2. Temperature dependence of the torsional constant of samples. Samples 1 and 2 are shown by empty circles and samples 3–10 by dark circles. Solid lines are the best fit according to the equation $\alpha(T) = \alpha_0 \cdot e^{-\Delta H^{\#}/RT}$.

tion occurs and the low absolute value of $\Delta H^{\#}$ seems to be correct. It must be remembered in fact that, at room temperature, the value of RT is about 2.51 kJ mol^{-1}. Some authors [6] explain the temperature dependence of α with the occurrence of premelting transitions, but as shown in Table 1 only the samples 1, 2 and 8, which contain at least three consecutive A bases, show premelting. Then, the $\Delta H^{\#}$ values that we measure are related to another temperature driven process, i.e. stacking variations. The values of $\Delta H^{\#}$ in Table 3 show a sequence dependence and sample no. 1, which contains mainly AA steps exhibits the lowest value. The same relation is valid also for the torsional constants.

As Fig. 2 shows, α varies both with the temperature and the sequence of the samples. In the range of temperature studied, the variation of α with the temperature is two- to three-fold, with the exception of sample no. 1 that, as mentioned, exhibits the lowest rigidity. In the figure the torsional rigidity constants of samples 1 and 3, marked with empty circles for a better visualization, are weakly affected by the temperature as compared to the other samples.

A comparison between the experimental α values extrapolated at 293 K for our samples and the α values predicted from their sequences has been attempted.

Torsional costants are related to the twist angle fluctuations of successive base pairs. By analysis of DNA crystal database, several authors [10–13] have derived twist angle values and their variance $\Delta\xi$ for the ten possible dinucleotide steps. The torsional constant can be easily calculated for each DNA sequence according to the relation

$$\alpha = k_B T/\Delta\xi^2$$

Table 3
Main hydrodynamic parameters, torsional constants at 293 K and enthalpy changes derived from FPA measurements

Sample	R_h (nm) ($\pm$0.02)	b (nm) ($\pm$0.01)	$\alpha\ 10^{-19}$ (J) ($\pm$0.2)	$-\Delta H^{\#}$ (kJ/mol)
1	1.09	0.34	2.3	9.2 $\pm$ 0.4
2	1.10	0.30	3.3	16.7 $\pm$ 0.8
3	1.10	0.29	3.6	11.7 $\pm$ 0.8
4	1.07	0.30	3.6	15.9 $\pm$ 1.2
5	1.13	0.32	3.9	16.3 $\pm$ 1.2
6	1.18	0.31	4.1	17.6 $\pm$ 0.8
7	1.08	0.32	4.2	17.6 $\pm$ 0.8
8	1.08	0.34	4.6	18.0 $\pm$ 1.3
9	1.08	0.32	5.0	18.0 $\pm$ 1.7
10	1.14	0.31	5.3	19.2 $\pm$ 0.8

where k_B is the Boltzmann constant and T the temperature expressed in K.

We have collected the values of base pair twist angle fluctuation $\Delta\xi$ for the ten possible dinucleotide steps recently calculated by four different groups [10–13] by the analysis of database of DNA crystals.

Suzuki and Yagi [10], in a study on DNA interaction with transcription factors, measured the twist standard deviations for 314 dinucleotide steps in 17 A and 16 B forms of DNA crystals. Terminal base steps were included in the calculation. Bhattacharyya et al. [12] studied the bending rigidity of DNA sequences correlated with the presence of cross-strand hydrogen bonds. Their study comprised 33 normal, 24 modified, 17 mismatched and two particular B-DNA sequences with the exclusion of unusual nucleotides. The total number of steps investigated was 644. Subirana and Faria [11] studied the influence of flanking sequences on the conformation of individual base steps in DNA. They analyzed 279 dinucleotide steps in 36 B DNA crystal structures excluding terminal base step from calculation. Liu and Beveridge [13] studied DNA bending models related to some dinucleotide step parameters. They studied 54 B DNA form crystals including among the others oligomers containing A-tracts with and without periodic helix phasing. The total number of steps investigated, including terminal base steps effects, was 496.

By using these four data sets we computed the torsional constant for the ten possible dinucleotide steps (α_{step}). The calculated α_{step} are reported in Fig. 3, ordered according to the relative increase of step rigidity. It is evident from the figure that there is a disagreement between the data of the four groups especially for the AC, AA, GA, GC and AT steps. This can be mainly due to the difference in DNA form studied, in the number of steps and criteria of step selection.

The mean torsional rigidity α_i has been computed according to the sequence of our samples with the equation: $1/\alpha_i = \Sigma\, 1/(n_{step}\alpha_{step})/26$, where n_{step} is the relative number of dinucleotide steps present in the sample, α_{step} is the α value of a dinucleotide step and 26 is the total number

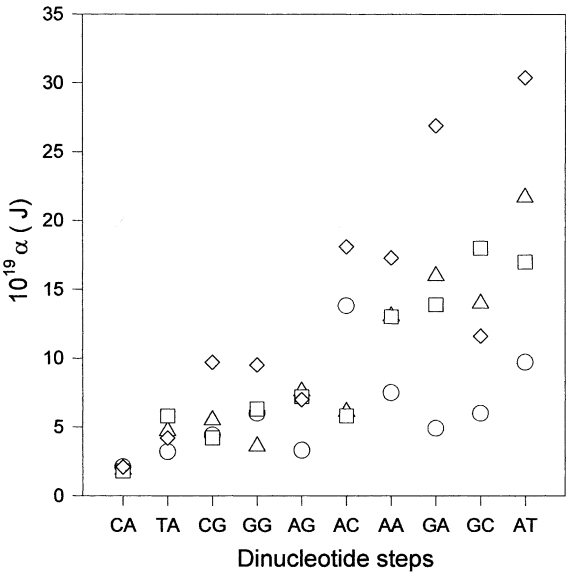

Fig. 3. Calculated α_{step} values for the ten possible dinucleotide steps of duplex DNA. Only one strand in 5′-3′ direction is shown for each step. (○) From Suzuki et al. [10]; (□) from Subirana et al. [11]; (△) from Bhattacharyya et al. [12]; (◇) from Liu et al. [13].

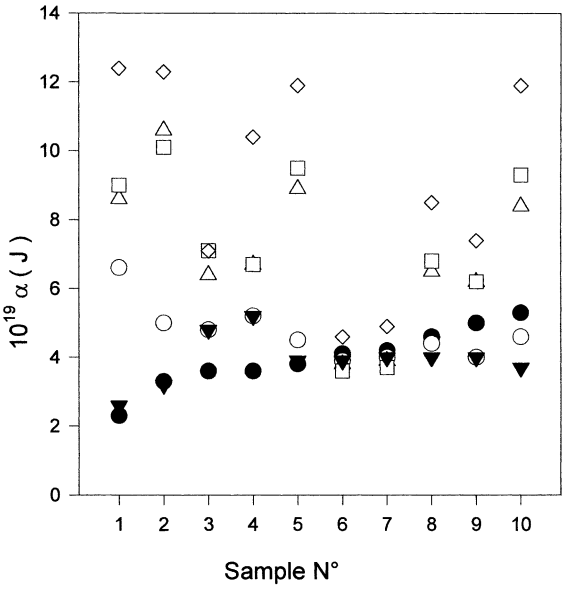

Fig. 4. Experimental and calculated torsional constants of the ten samples. (●) Experimental values; calculated values according to (○) Suzuki et al. [10]; (□) Subirana et al. [11]; (△) Bhattacharyya et al. [12]; (◇) Liu et al. [13], (▼) calculated as Suzuki with $\alpha_{AA} = 2.3 \times 10^{-19}$ J.

of steps. Fig. 4 shows the comparison between our experimental data of torsional rigidity with the α_i values calculated for each data set. The agreement between the α_i and the experimental ones is poor and the values derived by the crystal database in most cases overestimate our experimental values of rigidity. Only in the case of the samples 6 and 7 there is a good coincidence with all the three data sets but if we take into account the sequences of these samples it is evident that their torsional rigidity depends mainly on the presence of the dinucleotide steps AC, GC and AT (see Fig. 1 for the sequence). As shown in Fig. 3, these three latter dinucleotide steps are among the most rigid. From the same figure it is evident for the Suzuki and Yagi data [10] that the α_{CG} and α_{AT} values are lower in comparison to those of the three other data sets, whilst the α_{AC} are among the highest values. Therefore, it can be concluded that the coincidence of the fit is due to a compensating casual effect.

In Fig. 4 the best approximation between the four data sets and the FPA data is observed when the ten possible dinucleotide steps used to calculate the α_i are those derived by Suzuki and Yagi [10] (compare empty circles with dark circles). In this case the higher divergence between the data is observed for sample no. 1, the one rich in AA steps. By substituting the α_{AA} value of 7.5×10^{-19} J in the dinucleotide data set of Suzuki and Yagi [10] with the value of 2.3×10^{-19} J, equal to the experimental rigidity of sample no. 1, we have calculated new α_i values, that are reported in Fig. 4 as dark triangles. A better fit is now evident, so we suggest that the α_{AA} value of 2.3×10^{-19} J is a good estimate, in agreement with a recent theoretical study on DNA elasticity made by Lankas et al. [20], who obtained for the same step a torsional rigidity value equivalent to an α of 2.4×10^{-19} J.

Our results show an overestimation of the rigidity of the base pair steps derived by the analysis of DNA crystals. Packing forces of the lattice may immobilize the less rigid steps so that they, the most deformable, exhibit a lower value of standard twist deviation and, as a consequence, these steps are computed as the more rigid one. This overestimation is observed for the AA step as just discussed and is probably true also for AT and TA steps as can be deduced by comparison of the high values attributed to these steps (Fig. 3) with the experimental rigidity of sample no. 3 in Fig. 4. The same considerations extend to sample no. 4 in which, due to the large presence of CG or GC steps, the effect of the overestimation is evident. In the sample nos. 9 and 10 where steps AG and GA are prevalent, the rigidity values are underestimated.

The procedure by FPA analysis that we adopted for the measurement of the torsional constant values may be useful to determine more appropriate values for the ten possible dinucleotide steps. One drawback of this method could be represented by the lack of knowledge of the exact dye location. A good test might be lifetime measurements, as we have already shown in the case of the sample couple 6 and 7. In these two samples the invariance of the lifetime ensures that the dye resides in the same intercalation site. Then the variation of α could be unambiguosly attributed only to the single base substitution, which causes the change of two steps. However, only minor changes of α, within the experimental errors, are observed in this case, because the α value changes are averaged on 26 steps. The strategy of changing only one base at a time, in opportunely designed sequences, may be improved by the analysis of shorter samples. In the samples nos. 8 and 9 where two substitutions were introduced, the lifetime variation is indicative of a different intercalation site of the ethidium bromide. For these two samples, the changes of α cannot be unequivocally attributed to their step modifications. On the contrary the α value of 2.3×10^{-19} J estimated for the sample no. 1 is reliable.

4. Conclusions

In the 10–40 °C interval the DNA oligomers that we studied undergo to base stacking modifications. This effect is evidenced by the changes of

the elastic torsional properties and is associated to a $\Delta H^{\#}$ contribution that ranges from a minimum of 9.2 to 19.2 kJ mol^{-1}. This relative order of stability is related to the oligomer sequence, and generally to the α values too. These values are an estimate of the scale of variations in the elastic free energy that arises from variations in the base-pair sequence. Premelting transitions and base pair opening have been ruled out by our experiments due to the low energetic contribution measured, that never exceed the opening of one hydrogen bond. Although weak the $\Delta H^{\#}$ differences observed may be a signal, related to base sequence, for DNA–protein interactions. We have obtained a good agreement between the experimental torsional rigidities of our samples with those predictable on the basis of the dinucleotide steps derived by Suzuki and Yagi [10] with the assumption that the AA step has a lower value of α. The dinucleotide steps proposed by other authors [11–13] are probably overestimated, so that the rigidity evaluated for our sequences differs extensively from our experimental data. We observe that the main difference between Suzuki and Yagi's [10] and the other authors data [11–13] is due to the use in the calculation of both A and B-DNA form crystals, that is the most reliable situation also in solution where the real structure might be a mixture of different DNA forms.

Acknowledgements

We wish to thank Filip Lankas for the helpful discussions and suggestions during the preparation of this paper.

References

[1] D.P. Millar, R.J. Robbins, A.H. Zwail, Torsion and bending of nucleic acids studied by subnanosecond time-resolved fluorescence depolarization of intercalated dyes, J. Chem. Phys. 76 (1982) 2080–2093.

[2] J.M. Schurr, Rotational diffusion of deformable macromolecules with mean local cylindrical symmetry, Chem. Phys. 84 (1984) 71–76.

[3] M. Collini, G. Chirico, G. Baldini, M.E. Bianchi, Conformation of short DNA fragments by modulated fluorescence polarization anisotropy, Biopolymers 36 (1995) 211–225.

[4] G. Chirico, M. Collini, K. Toth, N. Brun, J. Langowski, Rotational dynamics of curved DNA fragments studied by fluorescence polarization anisotropy, Eur. Biophys. J. 29 (2001) 597–606.

[5] F. Barone, M. Matzeu, F. Mazzei, F. Pedone, Structural and dynamical properties of two DNA oligomers with the same base composition and different sequence, Biophys. Chem. 78 (1999) 259–269.

[6] J.J. Delrow, P.J. Heath, B.S. Fujimoto, J.M. Schurr, Effect of temperature on DNA secondary structure in the absence and presence of 0.5 M tetramethylammonium chloride, Biopolymers 45 (1998) 503–515.

[7] F. Barone, G. Chirico, M. Matzeu, F. Mazzei, F. Pedone, Triple helix oligomer melting measured by fluorescence polarization anisotropy, Eur. Biophys. J. 27 (1998) 137–146.

[8] F. Barone, F. Cellai, C. Giordano, M. Matzeu, F. Mazzei, F. Pedone, X-ray footprinting and fluorescence polarization anisotropy of a 30-mer synthetic DNA fragment with one 2′-deoxy-7-hydro-8-oxoguanosine lesion, Eur. Biophys. J. 28 (2000) 621–628.

[9] F. Barone, L. Cellai, M. Matzeu, F. Mazzei, F. Pedone, DNA, RNA and hybrid RNA–DNA oligomers of identical sequence: structural and dynamic differences, Biophys. Chem. 86 (2000) 37–47.

[10] M. Suzuki, N. Yagi, Stereochemical basis of DNA bending by transcription factors, Nucleic Acids Res. 23 (1995) 2083–2091.

[11] J.A. Subirana, T. Faria, Influence of sequence on the conformation of the B-DNA helix, Biophys. J. 73 (1997) 333–338.

[12] D. Bhattacharyya, S. Kundu, A.R. Thakur, R. Majumdar, Sequence directed flexibility of DNA and the role of cross-strand hydrogen bonds, J. Biomol. Struct. Dynam. 17 (1999) 289–300.

[13] Y. Liu, D.L. Beveridge, A refined prediction method for gel retardation of DNA oligonucleotides from dinucleotide step parameters: reconciliation of DNA bending models with crystal structure data, J. Biomol. Struct. Dynam. 18 (2001) 505–523.

[14] J. Sambrook, E.F. Fritsch, T. Maniatis, Molecular Cloning. A Laboratory Manual, Cold Spring Harbor Laboratory Press, Cold Spring Harbor, NY, 1989.

[15] C.R. Cantor, M.M. Warshaw, H. Shapiro, Oligonucleotide interaction. III Circular dichroism studies of the conformation of deoxyoligonucleotides, Biopolymers 9 (1970) 1059–1077.

[16] K.J. Breslauer, Extracting thermodynamic data from equilibrium melting curves for oligonucleotide order-disorder transitions, in: S. Agraval (Ed.), Methods in Molecular Biology, vol. 26. Humana Press, Totowa, NJ, pp. 347–372.

[17] S.A. Allison, M. Schurr, Torsion dynamics and depolarization of fluorescence of linear molecules. I. Theory and application to DNA, Chem. Phys. 41 (1979) 35–39.
[18] J.B. LePecq, C. Paoletti, A fluorescent complex between ethidium bromide and nucleic acids, Phys.-Chem. Characterization 27 (1967) 87–106.
[19] J.L. Bresloff, D.M. Crothers, Equilibrium studies of ethidium polynucleotide interactions, Biochemistry 20 (1981) 3547–53.
[20] F. Lankas, K. Sponer, P. Hobza, J. Langowski, Sequence-dependent elastic properties of DNA, J. Mol. Biol. 299 (2001) 695–709.